Artificial Neural Network Based Rotor Flux Estimation and Fuzzy-Logic Sensorless Speed Control of an Induction Motor

Tefera T. Yetayew(✉) and Rahel S. Sinta

Adama Science and Technology University, P.O. 1888, Adama, Ethiopia

Abstract. This paper aims to design rotor flux estimation based on artificial neural network (ANN) and fuzzy-logic based sensor less speed control of control for an induction motor drive. Induction motors are widely used for industrial applications with better reliability compared with DC-motor drives. However, control techniques for wide range speed control are complex. To achieve wide speed control range, field oriented control techniques are recommended. From the areas of application point of view, field sensors may not operate properly may be due to frequent failure that needs sensor less control technique. Thus, the research in this paper focuses on application of artificial neural network for flux estimation and fuzzy logic sensor less speed control of induction motor drive system. Performance evaluation of the control and flux estimation is done using MATLAB tool. The training of ANN for the flux estimation converged with epochs of 1000 and mean squared error of 0.00061617. The simulation results for the reference step input of 100 rad/s, the system with PI controller showed 5.851% percentage overshoot and 0.2 s settling time. Whereas the fuzzy based system resulted in 0.505% percentage overshoot and 0.085 s settling time. In summary, the controller performance reveals better dynamic response can be achieved using fuzzy logic based system than the system based on the conventional proportional integral (PI) controller.

Keywords: ANN · Fuzzy logic · Induction motor drive · Sensor less indirect field-oriented control

1 Introduction

Three-phase induction motor has been a reliable electromechanical energy conversion device for over 100 years. Induction motors, particularly the squirrel cage induction motors (SCIM) have been widely used in industrial applications because of their several inherent advantages such as their simple construction, robustness, reliability, low cost, and less maintenance needs [1]. The induction motor control methods are broadly classified into two categories i.e., scalar control and vector control. Scalar control: one of the primary ways of controlling induction motor was the Volts/Hertz speed control during which the motor was excited with constant voltage to frequency ratio to take care of a constant air gap flux and hence provide maximum torque sensitivity. This method is comparatively simple but doesn't yield satisfactory results for a high- performance application. This is often the fact that within the scalar control,

M. L. Berihun (Ed.): ICAST 2021, LNICST 411, pp. 288–303, 2022.
https://doi.org/10.1007/978-3-030-93709-6_19

an inherent coupling exists between the torque and air gap flux, which results in a sluggish response of the induction motor. Vector control (field-oriented control), overcome the limitation of the scalar control method [2, 3].

High performance vector control induction motor drives require speed or position information for its operation. However, these Sensors mounted on the machine shaft are not desirable for a variety of reasons. First of all, the cost is substantial. Secondly, their mounting requires a machine with two shaft ends available - one for the sensor and therefore the other one for the load coupling. Thirdly, electrical signals from the shaft sensor need to be taken to the controller and therefore the sensor needs an influence supply these require additional cabling. Finally, the presence of a shaft sensor reduces the mechanical robustness of the machine and its reliability [4–6]. Due to these reasons, speed sensor less systems, in which rotor speed measurements are not available, are preferred and find applications in many areas for speed regulation, load torque variation, and speed tracking purposes.

This paper addresses flux estimation technique using artificial neural network and speed control using fuzzy logic. And the contents are organized as dynamic models and control techniques in Sect. 2, flux estimation and controller design parts are presented in Sects. 3 and 4 respectively. The simulation results with the corresponding discussions and conclusions of findings in the research are presented in Sects. 5 and 6 respectively.

2 Dynamic Model of Induction Machine and Control Techniques

Assumptions made to produce mathematical model of the induction motor are summarized as follows:

- Copper loss is neglected.
- Spatial distribution of fluxes and amper turns wave are considered sinusoidal.
- Neglect all losses.
- Permeability of the rotor and stator are assumed infinite.

2.1 Dynamic Model of Induction Machine

Synchronous frame [7–10];

Equation (1) and (2) shows, the stator dq0 equations of voltage,

$$v_{ds}^{e} = R_s i_{ds}^{e} - \omega_e \varphi_{ds}^{e} + \frac{d\varphi_{ds}^{e}}{dt} \tag{1}$$

$$v_{qs}^{e} = R_s i_{qs}^{e} - \omega_e \varphi_{qs}^{e} + \frac{d\varphi_{qs}^{e}}{dt} \tag{2}$$

where v_{ds}^{e}, v_{qs}^{e} is stator voltages along d, q-axis respectively

Equation (3) and (4) shows, the rotor dq0 equations of voltage,

$$v_{dr}^{e} = R_r i_{dr}^{e} - (\omega_e - \omega_r)\varphi_{dr}^{e} + \frac{d\varphi_{dr}^{e}}{dt} \tag{3}$$

$$v_{qr}^{e} = R_r i_{qr}^{e} + (\omega_e - \omega_r)\varphi_{qr}^{e} + \frac{d\varphi_{qr}^{e}}{dt} \tag{4}$$

where v_{dr}^{e}, v_{qr}^{e} is rotor voltages along d, q-axis respectively.

Matrix form representation for the stator and rotor flux linkage is given by Eq. (5).

$$\begin{bmatrix} \varphi_{ds}^{e} \\ \varphi_{qs}^{e} \\ \varphi_{dr}^{e} \\ \varphi_{qr}^{e} \end{bmatrix} = \begin{bmatrix} L_s & 0 & L_m & 0 \\ 0 & L_s & 0 & L_m \\ L_m & 0 & L_r & 0 \\ 0 & L_m & 0 & L_r \end{bmatrix} \begin{bmatrix} i_{ds}^{e} \\ i_{qs}^{e} \\ i_{dr}^{e} \\ i_{qr}^{e} \end{bmatrix} \tag{5}$$

The torque developed in the q-axis current can be represented by Eq. (6),

$$T_e = \frac{3}{2}\frac{P}{2}\frac{L_m}{L_r}\left(\varphi_{rd} i_{sq} - \varphi_{rq} i_{sd}\right) \tag{6}$$

The mechanical system torque is given by Eq. (7),

$$T_e = J\frac{dw_r}{dt} + fw_r + T_L \tag{7}$$

where, w_r is rotor speed in RPM and J-is moment of inertia and f-friction coefficient.

2.2 Clark and Park Transformations

Clarke-park transformation transforms three-phase to two axis of α and β stationary and rotary by which complexity of analysis can be reduced [11].

A. Clarke transformation.
Equations (8)–(10) show the corresponding voltage expressions for an induction motor under unbalanced condition,

$$V_a = \sqrt{2} V_{rms} \sin(\omega t) \tag{8}$$

$$V_b = \sqrt{2} V_{rms} \sin(\omega t - \frac{2\pi}{3}) \tag{9}$$

$$V_c = \sqrt{2} V_{rms} \sin(\omega t + \frac{2\pi}{3}) \tag{10}$$

The result of clark transformation of V_{abc} to $V_{\alpha,\beta}$ is presented in Eq. (11),

$$\begin{bmatrix} V_\alpha \\ V_\beta \end{bmatrix} = \frac{2}{3}\begin{bmatrix} 1 & -\frac{1}{2} & -\frac{1}{2} \\ 0 & \frac{\sqrt{3}}{2} & -\frac{\sqrt{3}}{2} \end{bmatrix}\begin{bmatrix} V_a \\ V_b \\ V_c \end{bmatrix} \tag{11}$$

Equation (12) shows inverse Clark transformation results,

$$\begin{bmatrix} V_a \\ V_b \\ V_c \end{bmatrix} = \begin{bmatrix} 1 & 0 \\ -\frac{1}{2} & -\frac{\sqrt{3}}{2} \\ -\frac{1}{2} & -\frac{\sqrt{3}}{2} \end{bmatrix}\begin{bmatrix} V_\alpha \\ V_\beta \end{bmatrix} \tag{12}$$

B. Park transformation.
In the dq reference frame, Eq. (13) shows the system voltages,

$$\begin{bmatrix} V_d \\ V_q \end{bmatrix} = \begin{bmatrix} \cos(\theta) & \sin(\theta) \\ -\sin(\theta) & \cos(\theta) \end{bmatrix}\begin{bmatrix} V_\alpha \\ V_\beta \end{bmatrix} \tag{13}$$

Result of inverse park transformations results in,

$$\begin{bmatrix} V_\alpha \\ V_\beta \end{bmatrix} = \begin{bmatrix} \cos(\theta) & -\sin(\theta) \\ \sin(\theta) & \cos(\theta) \end{bmatrix}\begin{bmatrix} V_d \\ V_q \end{bmatrix} \tag{14}$$

2.3 Scalar Control of Induction Motor

Achieving wide speed control range like Dc motors for induction motor can be achieved by applying field oriented control techniques that may need relatively complex implementation of the controller but can provide the required control performance compared to scalar control approaches [3].

2.4 Field Oriented Control of Induction Motor

The field orientated control consists of controlling the stator currents represented by a vector. This control is based on projections that transform a three-phase time and speed-dependent system into a two co-ordinate (d and q co-ordinates) time-invariant system. These projections lead to a structure similar to that of a DC machine control. Field orientated controlled machines need two constants as input references: the torque component and the flux component [12]. There are two approaches to obtain the flux vector, one direct measurement, and the other is indirect. According to the field-oriented control can be classified as direct field orientation control (DFOC) and indirect field orientation control (IFOC).

A) Direct Field Oriented Control
The direct field-oriented control approach is based on by direct measurement of the air gap flux using appropriate sensor that is the hall effect sensor [14–17]. Schematic diagram in Fig. 1 shows the basic principle of how direct field oriented control technique operates.

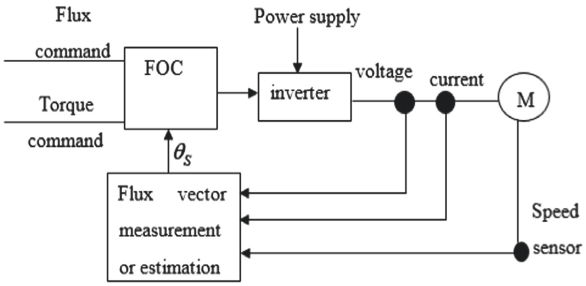

Fig. 1. Direct FOC method [17]

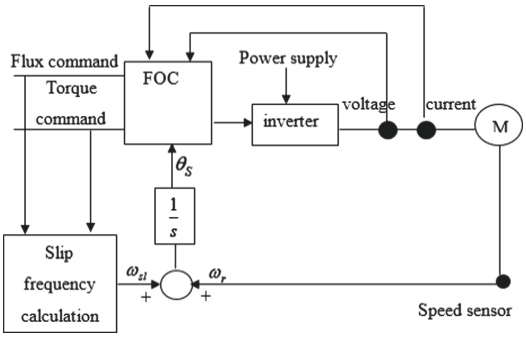

Fig. 2. Indirect FOC [17]

B) Indirect Field Oriented Control

Indirect field oriented approach computes the rotor flux by computing the slip speed [14, 17]. Figure 2 shows the schematic arrangement of the IFOC control approach.

The angular position, Θe, of the rotor flux vector is expressed as

$$\theta_e = \int \omega_e = \int (\omega_r + \omega_{sl}) \tag{15}$$

where, ω_r is the rotor speed, which is easy to measure using a shaft position sensor, and ω_{sl} is the slip frequency speed.

The procedures for indirect control approach can be summarized as follows [18]:

1. Stator current measurement and the required transformations.
2. Compute rotor angle using Eq. (15).
3. Error computation between the reference and rotor speed.
4. Quadrature current computation using Eq. (16),

$$I_{qs}^{*} = \left(\frac{2}{3}\right)\left(\frac{2}{P}\right)\left(\frac{L_r}{L_m}\right)\left(\frac{T_e^{*}}{\varphi_r}\right) \tag{16}$$

5. Compute the direct current component using Eq. (17),

$$I_{ds}^{*} = \frac{\lambda_r^{*}}{L_m} \tag{17}$$

where, λ_r^{*} is reference nominal flux linkage.

6. I_{ds}^{*} and I_{qs}^{*} are references for the current controller. The output of the current controller is the voltage. V_{ds}^{*} and V_{qs}^{*} voltage references are converted to $V_{\alpha s}^{*}$ and $V_{\beta s}^{*}$ using inverse park transformation and feed to SVPWM inverter to produce the inverter gating signals.

3 Flux and Speed Estimation for Sensor-Less IFOC of Induction Motor

3.1 Flux Estimation of the Three-Phase Induction Motor

Equations (18) and (19) show how to compute stator flux linkage [19].

$$\varphi_{ds}^{s,v} = \int \left(u_{ds}^{s} - i_{ds}^{s} R_s - u_{comp,ds}\right) dt \tag{18}$$

$$\varphi_{qs}^{s,v} = \int \left(u_{qs}^{s} - i_{qs}^{s} R_s - u_{comp,qs}\right) dt \tag{19}$$

Equations (20) and (21) are the expressions for rotor flux linkages,

$$\varphi_{dr}^{s,i} = \varphi_{dr}^{e,i} \cos\left(\theta_{\varphi r}\right) - \varphi_{qr}^{e,i} \sin\left(\theta_{\varphi r}\right) = \varphi_{dr}^{e,i} \cos\left(\theta_{\varphi r}\right) \tag{20}$$

$$\varphi_{qr}^{s,i} = \varphi_{qr}^{e,i} \cos\left(\theta_{\varphi r}\right) + \varphi_{dr}^{e,i} \sin\left(\theta_{\varphi r}\right) = \varphi_{dr}^{e,i} \sin\left(\theta_{\varphi r}\right) \tag{21}$$

where, $\theta_{\varphi r}$ is the rotor flux angle (rad).

Expressions (22) and (23) are for the compensated voltages,

$$u_{comp,ds} = K_p\left(\varphi_{ds}^{s,v} - \varphi_{ds}^{s,i}\right) + \frac{K_p}{T_i} \int \left(\varphi_{ds}^{s,v} - \varphi_{ds}^{s,i}\right) dt \tag{22}$$

$$u_{comp,qs} = K_p\left(\varphi_{qs}^{s,v} - \varphi_{qs}^{s,i}\right) + \frac{K_p}{T_i} \int \left(\varphi_{qs}^{s,v} - \varphi_{qs}^{s,i}\right) dt \tag{23}$$

Equations (24) and (25) are for rotor flux calculations,

$$\varphi_{dr}^{s,v} = -\left(\frac{L_s L_r - L_m^2}{L_m}\right) i_{ds}^{s} + \frac{L_r}{L_m} \varphi_{ds}^{s,v} \tag{24}$$

$$\varphi_{qr}^{s,v} = -\left(\frac{L_s L_r - L_m^2}{L_m}\right) i_{qs}^{s} + \frac{L_r}{L_m}\varphi_{qs}^{s,v} \tag{25}$$

Equation (26) is for rotor flux angle calculation on the voltage model,

$$\theta_{\varphi r} = \tan^{-1}\left(\frac{\varphi_{dr}^{s,v}}{\varphi_{qr}^{s,v}}\right) \tag{26}$$

The research in this paper applied artificial neural network for rotor flux estimation purpose by replacing the voltage and current models by which the voltage model will be less sensitive to variations of stator resistance and omit pure integrations. Application of ANN needs training data and in this research the training data set is generated using the current and voltage model equations.

3.2 Speed Estimation of the Three-Phase Induction Motor

Equation (27) shows the calculation for the synchronous speed,

$$W_e = \frac{d\theta_{\varphi r}}{dt} = \frac{1}{\left(\varphi_r^s\right)^2}\left(\varphi_{dr}^{s}\frac{d\varphi_{dr}^{s}}{dt} - \varphi_{qr}^{s}\frac{d\varphi_{qr}^{s}}{dt}\right) \tag{27}$$

The equation for rotor speed computation is given in Eq. (28),

$$\therefore w_r = w_e - \frac{L_m}{T_r}\left(\frac{\varphi_{dr}^{s} i_{qs}^{s} - \varphi_{qr}^{s} i_{ds}^{s}}{\left(\varphi_r^s\right)^2}\right) \tag{28}$$

where, $\frac{L_m}{T_r}\left(\frac{\varphi_{dr}^{s} i_{qs}^{s} - \varphi_{qr}^{s} i_{ds}^{s}}{\left(\varphi_r^s\right)^2}\right)$ is the slip.

3.3 Artificial Neural Network for Flux Estimation

Artificial neural network is a crude approximation of human network of neurons. In the artificial representation, training of neurons followed by the long term memory weight adjustment is required [20]. In this research, ANN is adapted for rotor flux estimation purpose using the required training data set and supervised learning. Figure 3 shows, the flow chart of application of ANN for the intended application in this paper.

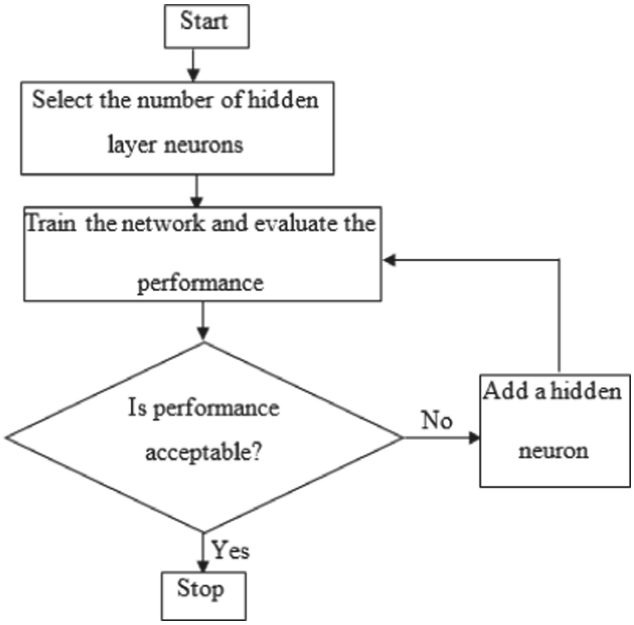

Fig. 3. Flow chart of the neural network training

The network structure in this paper with sigmoidal function as an activation function is given in Fig. 4.

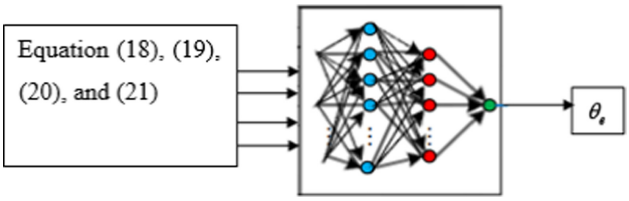

Fig. 4. Neural network structure

In this system the input layer, which is not neural, has 3 nodes; input layers, hidden layer, and output layer. The procedure to create and train a network using the toolbox is as follows:

- Training data sets of input and output are loaded in work space of MATLAB.
- Back propagation network comprise of four layers is created.
- Trainlim and Tansig were chosen as training and transfer function, respectively.
- Introduce training data set.
- Training parameters of convergence goal and epoach set.
- Training the system with data set and requirements set and evaluate the output.

Table 1 shows the required specifications for the induction motor considered in this paper.

Table 1. Induction motor parameters

Parameter	Symbol	Unit	Value
Types of rotor		_	Squirrel cage
Number of pole pairs	$\bar{p}$	_	2
Frequency	F	Hz	50
Stator resistance	R_s	Ω	0.966
Stator inductance	L_s	H	0.00439
Rotor resistance	R_r	Ω	1.45
Rotor inductance	L_r	H	0.00439
Mutual inductance	L_m	H	0.002373
Moment of inertia	J	kgm^2	0.009
Rated voltage	V_r	v	400
Rated speed	ω_r	RPM	1460
Rated power	P_r	KW	2.2
Friction factor	F	N.m.s	0.00061
PWM frequency	Fs	KHz	20

The training results given in Fig. 5 shows 1000 epoach with the convergence value of 0.00061617.

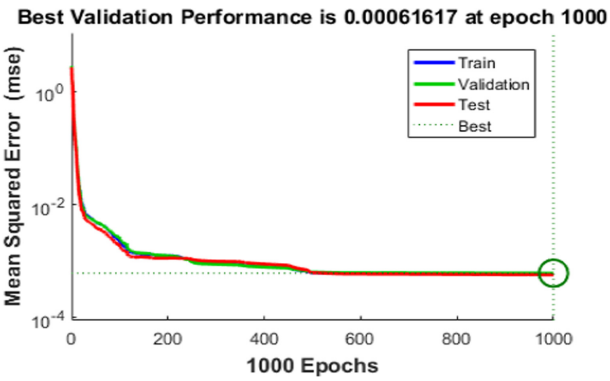

Fig. 5. Validation of the mean squared error

4 Design of PI and Fuzzy Logic Speed Controller

In this research, the controller is based on fuzzy logic algorithm with ANN for flux estimation application. To evaluate the performance of fuzzy based controller, PI based controller is designed and evaluated along with.

4.1 Designing a Proportional-Integral (PI) Controller

Conventional controllers of PID type are widely in use for different applications being simple in implementation and design the required constants of the controller. There various approaches of determining the required parameter values of a conventional PID controller. These can be analytical, manual tuning and application of auto-tuning approach using appropriate computation tool [21]. Block diagram representation of a typical PID controller is presented in Fig. 6.

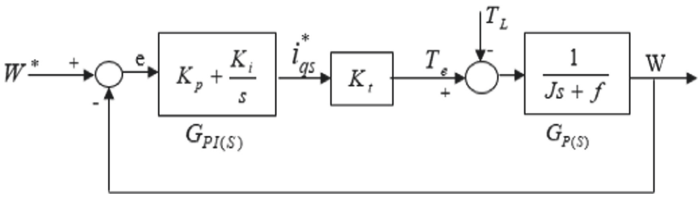

Fig. 6. Model of Speed PI Controller block diagram

where W^* is the reference rotor angular speed, W is the rotor angular speed, $e = W^* - W$ is the tracking speed error, K_P is the proportional gain of speed, K_i is the integral gain, f is the total damping coefficient, T_L is load torque, K_t denotes torque constant, T_e denotes the electromagnetic torque. From Fig. 8.

$$T_e = K_t i_{qs}^* \tag{29}$$

$$i_{qs}^* = \frac{2}{3} * \frac{2}{p} * \frac{L_r}{L_m} * \frac{T_e}{\varphi_r} \tag{30}$$

$$\phi_r = L_m i_{ds} \tag{31}$$

From Eqs. (29)–(31) K_t is given by:

$$K_t = \left(\frac{3pL_m^2}{4L_r}\right) i_{ds}^* \tag{32}$$

The parameters K_P and K_i of the continuous controller are obtained by the following steps;

Step 1: Open loop transfer function.
Step 2: Controller parameters for the closed loop system.

Equation (33) shows the open-loop transfer function of the system at no load condition.

$$Go(s) = G_{PI}(s) \times G_P(s) = K_t\left(\frac{sK_P + K_i}{Js^s + sf}\right) \tag{33}$$

Equation (34) shows the closed loop system transfer function,

$$G_C(s) = \frac{G_O(s)}{1 + H(s)G_O(s)} = \frac{\frac{K_t}{J}\left(sK_p + K_i\right)}{s^2 + \left(\frac{f + K_t K_p}{J}\right)s + \frac{K_t K_i}{J}} \tag{34}$$

By comparing with a second order closed loop transfer function and setting $\xi = 1$, values of the PI controller are computed and presented in Table 2.

Table 2. Proportional (K_P) and Integral (K_i) gain for PI controller

PI controller	**Kp**	**Ki**
Speed control loop	2	563
Inner $d_e - q_e$ current loops	0.135	265.09

4.2 Designing Fuzzy Logic Speed Controller

Artificial intelligence based algorithms such as ANN and fuzzy logic have better capability in handling non-linearity compared with classical algorithms. However, implementation complexity and more computation requirement are major draw backs of intelligent algorithms. Fuzzy based controller is to model the operator knowledge for control application having basic procedures of fuzzification, rule base, inference and defuzzification activities as shown in Fig. 7 [22, 23].

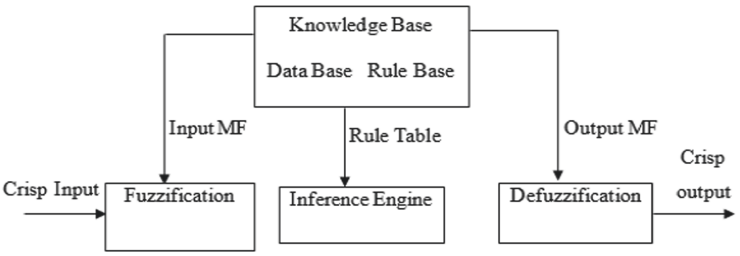

Fig. 7. Basic structure of the fuzzy logic controller

In this research, the fuzzy based controller comprises of two inputs of error and change is error and one output. Triangular member ship function of seven variables for both inputs and output and mamdani based inference is considered. Plot of membership functions and the rule table are summarized in Fig. 8.

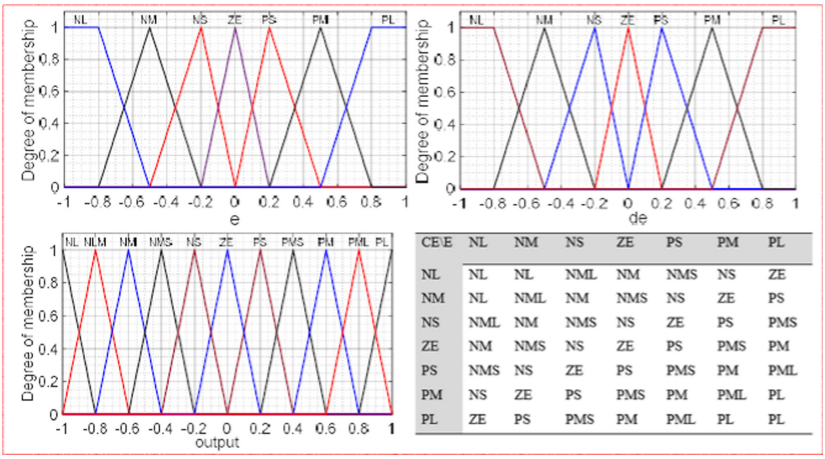

CE\E	NL	NM	NS	ZE	PS	PM	PL
NL	NL	NL	NML	NM	NMS	NS	ZE
NM	NL	NML	NM	NMS	NS	ZE	PS
NS	NML	NM	NMS	NS	ZE	PS	PMS
ZE	NM	NMS	NS	ZE	PS	PMS	PM
PS	NMS	NS	ZE	PS	PMS	PM	PML
PM	NS	ZE	PS	PMS	PM	PML	PL
PL	ZE	PS	PMS	PM	PML	PL	PL

Fig. 8. Membership functions of input error (e), change in error (de), output and rule table.

5 Results and Discussions

Schematic diagram of the system for implementation in MATLAB/Simulink is given in Fig. 9.

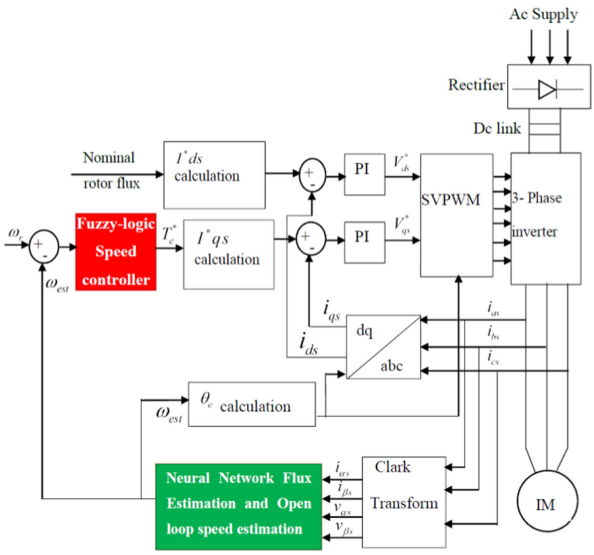

Fig. 9. Schematic diagram of the proposed system

The simulation results of the proposed sensorless speed control of indirect field-oriented control of induction motor drive are discussed in terms of:

- Space vector pulse width modulation.
- Setpoint tracking capability.
- Step response at no load.
- Step response when loaded.

The equivalent space-vector modulations of waveforms spaced 1200 is given in Fig. 10.

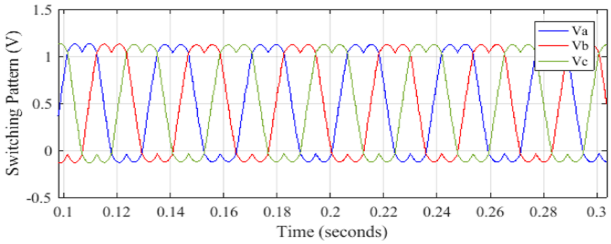

Fig. 10. Voltage for three phases (PWM Duty cycles)

Figures 11, 12 and 13 shows the estimated parameters of the motor.

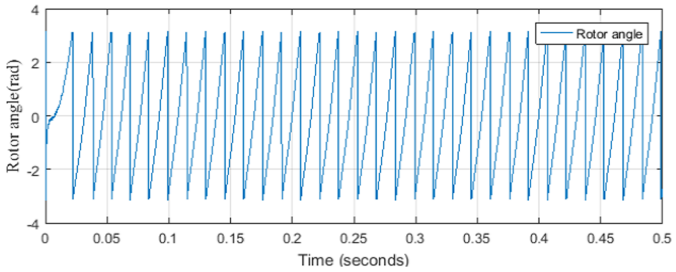

Fig. 11. Estimated rotor flux angle vs time

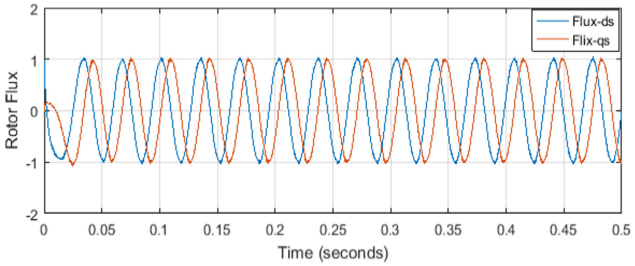

Fig. 12. Estimated rotor flux in dq-axis reference frame vs time

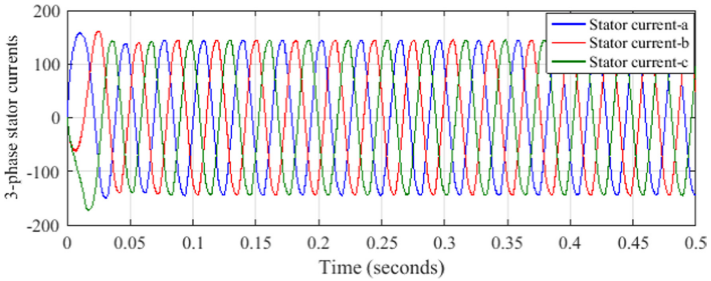

Fig. 13. Three-phase stator current vs time at 100 rad/s.

The angle of rotor flux to the stationary frame d-axis is estimated with the proposed flux linkages in the rotating reference frame are found by using voltage and current flux estimation and then the rotor flux angle improved by using an artificial neural network. The estimated rotor flux with a reference speed of 100 rad/s is shown as in Fig. 12. Both the dq-axis fluxes are 90-degree out of phase.

Three phase stator currents generated using voltage source inverter are given in Fig. 13. The three phase currents are equal and 120° phase displaced generated using the voltage source inverter controlled using space vector modulation technique.

At the same time the controllers' performance for the reference set point of 100 rad/s at no-load condition is presented in Fig. 14.

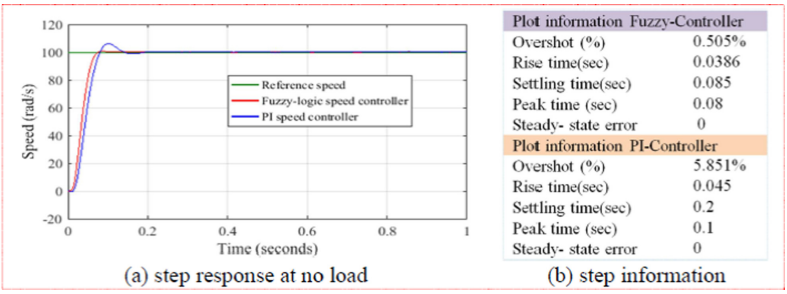

Plot information Fuzzy-Controller	
Overshot (%)	0.505%
Rise time(sec)	0.0386
Settling time(sec)	0.085
Peak time (sec)	0.08
Steady- state error	0
Plot information PI-Controller	
Overshot (%)	5.851%
Rise time(sec)	0.045
Settling time(sec)	0.2
Peak time (sec)	0.1
Steady- state error	0

Fig. 14. PI and fuzzy logic speed controller Vs time for 100 rad/s at no-load condition

From the control system theory, the system is said to have better dynamic performance if it has a lower rise time, lower percent overshoot, lower settling time, and lower peak time. The PI speed controller has poor performance than the fuzzy logic speed controller. It has a 5.851% overshoot and settling time of 0.2 s. The fuzzy logic controller has a better result in the case of overshoot (0.505%) and settling time (0.085 s) than the PI controller. The system response at load of 5Nm with reference set point of 100 rad/s is given in Fig. 15. The dynamic measurement criterion are also presented in the right side of the simulation result, Fig. 15(b).

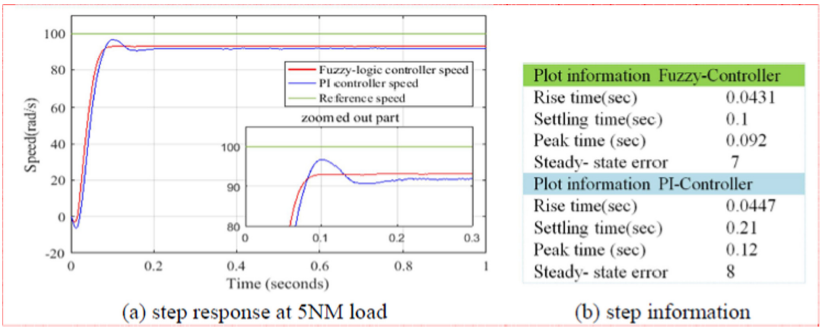

Plot information Fuzzy-Controller	
Rise time(sec)	0.0431
Settling time(sec)	0.1
Peak time (sec)	0.092
Steady- state error	7
Plot information PI-Controller	
Rise time(sec)	0.0447
Settling time(sec)	0.21
Peak time (sec)	0.12
Steady- state error	8

Fig. 15. PI and fuzzy logic speed controller vs time for 100 rad at (5 NM) load condition

The settling time, rise time, and peak time values are increased when compared to the system simulated under no-load condition. This shows that when the load is increased the system performance will be decreased. There is no variation in the case of overshoot but there is a steady-state error in the result with the system simulated under no-load condition.

6 Conclusion

In this research, flux estimation is done using artificial neural network and the sensor less speed control of the induction motor based on indirect field-oriented control is done with fuzzy logic. The performance of speed control of the indirect vector control of an induction motor using conventional PI and Fuzzy control has been compared. Accordingly, the PI speed controller has a settling time 0.2 s, 5.851% overshoot, 0.045 s rise time, 0.1 s peak time, and 0% steady-state error for 100 rad/s at no-load condition. On the other hand, the fuzzy logic speed controller has a settling time of 0.085 s, 0.505% overshoot, 0.0386 s rise time, and 0% steady-state error for 100 rad/s at no-load condition. Thus, values show that the fuzzy-logic based speed control of indirect vector control of induction motor gives a better speed response than that of the conventional PI controller at no-load condition. The performance of PI and fuzzy-logic controller evaluated under the application of sudden load (5 Nm) change and constant set point condition for both performed control systems. The settling time, rise time, and peak time values are increased when compared to the system simulated under no-load condition. This shows that when the load is increased the system performance will be decreased. There is no variation in the case of overshoot but there is a steady-state error.

References

1. Rashid, M.H.: Power Electronics Devices Circuits and Applications, 4th edn. (2014)
2. Fitzgerald, A.E.: Electrical Machine, 6th edn. (5 March 2006)

3. Mohan, N.: Advanced Electric Drives, 2nd edn. Wiley, Hoboken, New Jersey (2014)
4. Filippich, M.: Digital Control of Three Phase Introduction Motor, Thesis University of Queensland (October 2002)
5. Li, M.: A Differential-Algebric Approach to Speed and Parameter Estimator of Induction, Thesis University of Tennessee (2005)
6. Chapman, S.J.: Electric Machinery Fundamentals, 5th edn. (2004)
7. Blaschke, F.: The principle of field orientation as applied to the new trans-vector closed loop control systems for rotating machines. Siemens Rev. **39**(5), 217–220 (2001)
8. Chourasia, A., Srivastava, V., Choudhary, A., Praliya, S.: Comparison study of vector control of induction motor using rotor flux estimation by two different methods. Int. J. Electr. Electr. Eng. **7**(3), 201–206 (2014)
9. Mishra, A., Choudhary, P.: Speed control of an induction motor by using indirect vector control method. Int. J. Emerg. Technol. Adv. Eng. **2**(12), 144–150 (2012)
10. Campbell, S., Toliyat, H.A.: DSP-Based Electromechanical Motion Control. CRC Press (2004)
11. Krouse, P.C., Wasynczuk, O., Sudhoff, S.D.: Analysis of Electric Machinery and Drive Systems. Wiley, United States of America (2002)
12. Kazmierkowski, M.P., Krishnan, R., Blaabjerg, F.: Control in Power Electronics Selected Problems. Acadamic Press (2002)
13. Popescu, M.: Induction motor modeling for vector control purposes. Laboratory of Electromechanics, Department of Electrical and Communications Engineering, Helsinki University of Technology (2000)
14. Bose, B.K.: Modern Power Electronics and AC Drives, 4th edn. Pearson Education (2004)
15. Umanand, L., Bhat, S.: Online estimation of stator resistance of an induction motor for speed control applications. IEE Proc. Electr. Power Appl. **142**, 97–103 (2001)
16. Zhang, P., Lu, B., Habetler, T.G.: A remote and sensorless stator winding resistance estimation method for thermal protection of soft-starter-connected induction machines. IEEE Trans. Ind. Electr. **55**(10), 3611–3618 (2008)
17. Gopal, B.T.V.: Comparison between direct and indirect field oriented control of induction motor. Int. J. Eng. Trends Technol. **43**, 364–369 (2017)
18. Kassa, G.: Design and comparative analysis of genetic algorithm tuned fractional and integer order PI controllers with adaptive neuro fuzzy controller for speed control of indirect vector controlled induction motor. Addis Ababa Institute of Technology (January 2019)
19. Hambissa, T.: Analysis and DSP implementation of sensor-less direct FOC of three-phase induction motor using open-loop speed estimator. Addis Ababa Institute of Technology (17 May 2017)
20. Sonawane, P.P., Joshi, S.D.: Sensorless speed control of induction motor by artificial neural network. Int. J. Ind. Electr. Electr. Eng. **5**(2), 2347–6982 (2017)
21. Mhaisgawali, M.L.: Speed control of induction motor using PI and PID controller. IOSR J. Eng. **03**(05), 25–30 (2013)
22. Mishra, A., Zaheeruddin: Design of speed controller for squirrel-cage induction motor using fuzzy logic based techniques. Int. J. Comput. Appl. **58**(22), 10–18 (2012)
23. Hamood, M.A., Faris, W.F., Badran, M.A.: Fuzzy logic based speed control system for three phase induction motor. EFTIMIE MURGU (2013). ISSN 1453-7397